The Shu Complex Prevents Mutagenesis and Cytotoxicity of Single-Strand Specific Alkylation Lesions

Braulio Bonilla[1], Alexander J. Brown[2], Sarah R. Hengel[1], Kyle S. Rapchak[1], Debra Mitchell[2], Catherine A. Pressimone[1], Adeola A. Fagunloye[1], Thong T. Luong[1], Hani S. Zaher[3], Nima Mosammaparast[4], Ewa P. Malc[5], Piotr A. Mieczkowski[5], Steven A. Roberts[2,#], Kara A. Bernstein[1,#]

[1]University of Pittsburgh, School of Medicine, Department of Pharmacology and Chemical Biology, Pittsburgh, PA 15213, USA.

[2]Washington State University, School of Molecular Biosciences and Center for Reproductive Biology, College of Veterinary Medicine, Pullman, WA 99164, USA.

[3]Washington University in St. Louis, Department of Biology, St. Louis, MO 63130, USA

[4]Washington University in St. Louis, Department of Pathology and Immunology, St Louis, MO 63110, United States of America.

[5]Department of Genetics, Lineberger Comprehensive Cancer Center, University of North Carolina, Chapel Hill, NC 27599, USA.

[#]Corresponding authors:

Kara A. Bernstein, karab@pitt.edu

Steven A. Roberts, steven.roberts2@wsu.edu

ABSTRACT

Three-methyl cytosine (3meC) are toxic DNA lesions, blocking base pairing. Bacteria and humans, express members of the AlkB enzymes family, which directly remove 3meC. However, other organisms, including budding yeast, lack this class of enzymes. It remains an unanswered evolutionary question as to how yeast repairs 3meC, particularly in single-stranded DNA. The yeast Shu complex, a conserved homologous recombination factor, aids in preventing replication-associated mutagenesis from DNA base damaging agents such as methyl methanesulfonate (MMS). We found that MMS-treated Shu complex-deficient cells, exhibit a genome-wide increase in A:T and G:C substitutions mutations. The G:C substitutions displayed transcriptional and replicational asymmetries consistent with mutations resulting from 3meC. Ectopic expression of a human AlkB homolog in Shu-deficient yeast rescues MMS-induced growth defects and increased mutagenesis. Finally, the Shu complex exhibits increased affinity for 3meC-containing DNA. Thus, our work identifies a novel mechanism for coping with alkylation adducts.

INTRODUCTION

Alkylating agents such as methyl methanesulfonate (MMS) induce a diverse set of base lesions that are recognized and repaired by the base excision repair (BER) pathway or direct repair enzymes such as the AlkB family (Fu, Calvo et al., 2012, Yi & He, 2013). However, when these lesions, or its repair intermediates, are encountered by a replisome, replication fork stalling can occur (Shrivastav, Li et al., 2010, Sobol, Kartalou et al., 2003). In this scenario, DNA base damage is preferentially bypassed using homologous recombination (HR) or translesion synthesis (TLS), postponing its repair but allowing replication to be completed in a timely

fashion. These pathways are often referred to as post-replication repair (PRR) or DNA damage tolerance (DDT) and are best described in the budding yeast *Saccharomyces cerevisiae* (Arbel, Liefshitz et al., 2020, Boiteux & Jinks-Robertson, 2013, Ulrich, 2007).

In yeast, HR-mediated PRR is an error-free pathway and is dependent on the polyubiquitination of PCNA by the Mms2-Rad5-Ubc13 complex (Arbel et al., 2020). Lesion bypass is achieved by Rad51 filament formation, and recombination between sister chromatids to fill the single-stranded DNA (ssDNA) gaps originated from the stalling of replicative polymerases. While HR can bypass these lesions in an error-free manner, TLS can also bypass this damage. However, TLS may lead to mutations and is often referred as error-prone lesion bypass. In yeast, TLS serves as an alternative pathway to error-free lesion bypass, as disruption of genes involved in the error-free PRR pathway leads to increased mutations that is dependent on TLS (Broomfield, Chow et al., 1998, Huang, Rio et al., 2003, Swanson, Morey et al., 1999).

The study of the error-free PRR pathway is challenging due to the diverse roles of HR proteins in additional processes, such as DSB repair. The Shu complex is an evolutionarily conserved HR factor that we recently discovered to function in strand-specific DNA damage tolerance during replication and thus provides an excellent model to specifically study HR proteins in the context of PRR (Godin, Meslin et al., 2015, Godin, Sullivan et al., 2016b, Martino & Bernstein, 2016, Rosenbaum, Bonilla et al., 2019). In *S. cerevisiae*, the Shu complex is a heterotetramer formed by the SWIM domain-containing protein, Shu2, and the Rad51 paralogs, Csm2, Psy3, and Shu1. The Shu complex promotes Rad51 filament formation, a key step for HR (Godin et al., 2016b). Consistent with their role in DSB repair, most HR genes deletions lead to increased sensitivity to DSB-inducing agents. However, this is not the case with the Shu complex, as its mutants are primarily sensitive to the alkylating agent MMS, but not to the DSB

68 inducing agents such as ionizing radiation (Godin, Zhang et al., 2016c, Shor, Weinstein et al.,
69 2005). This makes the Shu complex attractive to dissect the role of HR in the tolerance of
70 replication-associated DNA damage.

71 Previous studies from our group and others demonstrated that the Shu complex operates
72 in the error-free branch of the PRR to tolerate DNA damage from MMS-induced lesions (Ball,
73 Zhang et al., 2009, Godin, Wier et al., 2013). Despite these findings, it has remained unknown
74 which MMS-induced lesions, or repair intermediates, the Shu complex is important for. Our
75 previous results uncovered genetic interactions between factors of the BER pathway and the Shu
76 complex upon MMS treatment (Godin et al., 2016c). Notably, cells lacking the BER abasic (AP)
77 endonucleases and AP lyases that process AP sites exhibit exquisite sensitivity towards
78 alkylating agents and display a three order of magnitude increase in mutations rates when the
79 Shu complex is disrupted. We recently demonstrated that the Shu complex is important for
80 tolerance of AP sites (Rosenbaum et al., 2019). However, it remains outstanding question as to
81 whether the Shu complex may recognize other MMS-induced fork blocking lesions.

82 Here, we addressed whether the Shu complex function is specific for AP sites or if it is
83 important for recognition of a broader range of DNA lesions. To do this, we performed whole
84 genome sequencing of Shu mutant cells (i.e. *csm2*Δ) that had been chronically exposed to MMS.
85 In turn, this allowed us to obtain an unbiased spectrum of mutations the Shu complex helps to
86 mitigate. We determined that the Shu complex prevents mutations at both A:T and C:G base
87 pairs. However, transcriptional and replicative asymmetries in C:G mutations suggest a novel
88 role for the Shu complex in the tolerance of 3meC, in addition to AP sites. Importantly, unlike
89 bacteria and human cells that have an enzyme that directly repairs 3meC, this family of enzymes
90 is absent in *S. cerevisiae* and therefore it has remained unknown how 3meC are repaired in yeast

(Sedgwick, Bates et al., 2007). Our data suggest that the Shu complex is important for 3meC tolerance. Indeed, expression of human *ALKBH2*, responsible for 3meC repair, specifically rescues the MMS-sensitivity of Shu-complex mutant cells and alleviates their MMS-induced mutagenesis. In contrast to Shu complex mutants, we observe that *ALKBH2* expression very weakly rescues the MMS sensitivity associated with HR deletion strains. Finally, we find that the Shu complex DNA-binding subunits, Csm2-Psy3, have higher affinity for double-flap substrates containing 3meC relative to an unmodified substrate. Altogether, our findings reveal a previously unappreciated role for the Shu complex in mediating damage tolerance of 3meC in single-stranded DNA, finally uncovering how yeast tolerate these highly toxic lesions. Additionally, the ability of the Shu complex to facilitate tolerance of 3meC DNA damage through homology-directly bypass likely highlights an important repair pathway for these lesions even in organisms that express AlkB homologs.

RESULTS

Unbiased genome-wide analysis of mutation patterns suggests that the Shu complex function in the error-free bypass of specific MMS-induced lesions

To determine the identity of MMS-induced lesions that the Shu complex helps the replication fork to bypass, we chronically exposed Shu complex-deficient cells to MMS. In particular, wild-type (WT) or *csm2*Δ cells were plated on MMS-containing medium and then individual colonies were transferred every two days onto fresh medium containing 0.008% MMS, for a total of ten passages. We then extracted genomic DNA from these colonies and performed whole-genome sequencing to measure mutation frequencies. Consistent with previous

findings, *csm2*Δ cells accumulated a median 12.7-fold more mutations than WT upon MMS treatment (**Figure 1A**) (Godin et al., 2013, Godin et al., 2016c). To infer which DNA lesions caused the mutations, we analyzed the substitution patterns considering the MMS-induced lesion profile (Beranek, 1990, Sikora, Mielecki et al., 2010, Wyatt & Pittman, 2006). 3meA is the most common MMS-induced lesion at A:T base pairs in dsDNA and can itself be mutagenic or converted to a mutagenic AP site by the Mag1 glycosylase or by spontaneous depurination (**Figure 1B** and **1C**) (Shrivastav et al., 2010). When these AP sites are encountered by a replicative polymerase, they can lead to its stalling. TLS activity on 3meA-derived AP sites leads to an A->G and A->T substitution pattern (**Figure 1C**) due to the tendency of Rev1 or the replicative polymerase δ incorporating a C or A on AP sites, respectively (**Figure 1C**) (Chan, Resnick et al., 2013, Haracska, Unk et al., 2001, Hoopes, Hughes et al., 2017). Consequently, most substitutions at A:T bases in MMS-treated WT yeast A to G and A to T (**Figure 1B**). Previous analyses of MMS-treated *mag1*Δ yeast revealed that deletion of the glycosylase responsible for initiating base excision repair of 3meA resulted in a mutation spectrum also predominantly composed of A to G and A to T substitutions (Mao, Brown et al., 2017), indicating that these two mutation types are likely directly induced by 3meA as opposed to 3meA-derived AP sites. MMS-treated *csm2*Δ cells (**Figure 1B**) displayed elevated A->G transitions and A->T transversions, consistent with a function for the Shu complex in the bypass of 3meA or 3meA-derived AP sites, as we recently demonstrated (Godin et al., 2016c, Rosenbaum et al., 2019).

7meG is the most common MMS-induced DNA adduct at G:C base pairs and is not itself mutagenic (Shrivastav et al., 2010). However, it is eliminated by spontaneous depurination, or Mag1 excision, which both lead to AP sites (Bjoras, Klungland et al., 1995, Shrivastav et al.,

2010, Wyatt, Allan et al., 1999). When AP sites are generated from guanines, their bypass by Rev1 is error-free because it incorporates a C across the missing base. Alternatively, bypass by the replicative polymerase results in the incorporation of A across the missing base, which leads to a G to T transversion (**Figure S1**). Interestingly, the MMS-induced mutation profile at G:C base pairs in WT yeast, not only includes G->T mutations but also high levels of G->A and G->C mutations (**Figure 1D**), suggesting that 7meG-derived AP sites are unlikely to cause these mutations. Deletion of *CSM2* results in a similar spectrum of MMS-induced G:C substitutions compared to that observed in WT yeast, but at elevated frequency, indicating that the Shu complex mediates tolerance of the same MMS-induced lesion that contributes to G:C base pair mutagenesis in WT cells, possibly N3-methylcytosine (3meC). 3meC is a mutagenic DNA adduct predominantly induced by MMS at ssDNA and can block the replicative polymerase (Shrivastav et al., 2010). Rev3-mediated TLS bypass of 3meC leads to the incorporation of a random nucleotide across the lesion, leading to a mutational pattern consistent with the one we observed in WT and *csm2*Δ yeast (**Figure 1E**) (Saini, Sterling et al., 2020, Yang, Gordenin et al., 2010), indicating that the Shu complex may also bypass this ssDNA specific alkylation lesion.

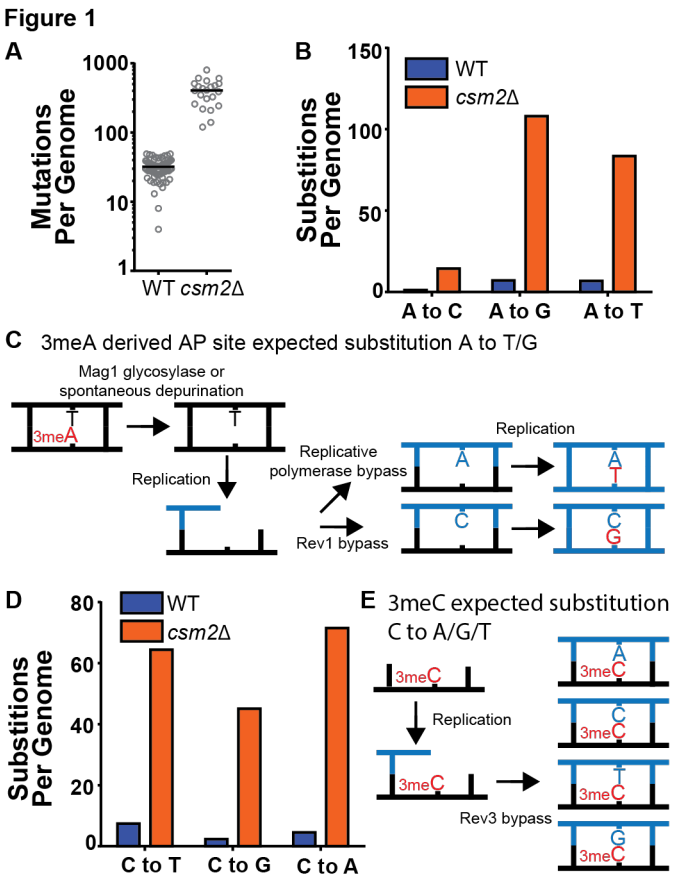

Figure 1. *csm2Δ* Cells Chronically Exposed to MMS Exhibit Substitution Patterns Consistent with TLS Activity Bypassing AP Sites and 3meC

WT and *csm2*Δ cells were chronically exposed to MMS. WT and *csm2*Δ cells were chronically exposed to 0.008% MMS by plating individual colonies onto rich medium containing MMS, after 2 days of growth, the colonies were platted onto fresh medium containing MMS for 10 passages. DNA was extracted from 90 colonies per genotype and deep sequenced.

(A) The number of mutations per genome for WT or *csm2*Δ cells chronically MMS-exposed. Horizontal bar indicates the median value for each genotype.

(B) The average number of each type of A:T substitution per genome in MMS-treated WT and *csm2*Δ cells.

(C) Schematic of how 3meA derived AP sites result in A to T/G mutations. 3meA is removed by the Mag1 glycosylase or spontaneously depurinated resulting in an AP site. During DNA replication, the replicative polymerase bypasses the AP site resulting in a T mutation or alternatively Rev1 bypasses the AP site resulting in a G mutation.

(D) The average number of each type of G:C substitution per genome in MMS-treated WT and *csm2*Δ cells.

(E) Schematic of how 3meC results in C to A/G/T base substitutions. 3meC occurs primarily in ssDNA and during replication, Rev3 mediated bypass results in incorporation of A, T, G, or C nucleotides.

DNA lesions that arise at ssDNA often result in mutation patterns that exhibit strand bias

near origins of replication and at highly transcribed genes (Roberts, Sterling et al., 2012, Saini & Gordenin, 2020). Additionally, lesions subject to preferential repair of the transcribed DNA strand by transcription-coupled nucleotide excision repair (TC-NER) can also display transcriptional asymmetry (i.e. having higher mutation densities on the non-transcribed strand compared to the transcribed stand). We therefore evaluated whether mutations from our whole genome sequenced yeast displayed either transcriptional or replicative asymmetry (**Figure 2**). A:T mutations in both MMS-treated WT and *csm2Δ* yeast showed very little replicative asymmetry, but displayed transcriptional asymmetry, similar to that seen in MMS-treated *mag1*Δ yeast (Mao et al., 2017). The transcriptional asymmetry of A:T mutations in MMS-treated *mag1*Δ yeast results from TC-NER activity on unrepaired 3meA, indicating that the Shu complex may help prevent mutations associated with 3meA (Beranek, 1990, Sikora et al., 2010, Wyatt & Pittman, 2006). However, increased mutagenesis of the minor ssDNA specific lesion N1-methyl adenine (1meA) would also be expected to produce higher mutation densities on the non-transcribed strand. Therefore, we cannot exclude the possibility that 1meA contributes to the increased MMS-induced mutation rate in *csm2Δ* cells. G:C mutations in MMS-treated WT yeast displayed little to no transcriptional or replicative strand asymmetry, while the same mutations in MMS-exposed *csm2*Δ cells exhibited both types of strand bias (**Figure 2**). The transcriptional asymmetry displayed higher densities of C mutations on the non-transcribed strand, consistent with either TC-NER removal of 3meC or preferential formation of 3meCs on the transiently ssDNA non-transcribed strand, instead of an asymmetry derived for TC-NER of 7meG. We additionally note that transcriptional asymmetry of the 3meC in MMS-treated *csm2*Δ extends up to 167 bp upstream of the transcriptional start site. This may suggest that either TC-NER can function within this region or some ssDNA is assessable on the non-transcribed strand due to the

195 binding of TFIIH to the promoter region upstream of the TSS. Likewise, replicative asymmetry
196 indicated elevated C mutations associated with the lagging strand template across the yeast
197 genome, suggesting that 3meC lesions formed during lagging strand synthesis are bypassed in an
198 error-free manner in Shu proficient yeast.

Figure 2

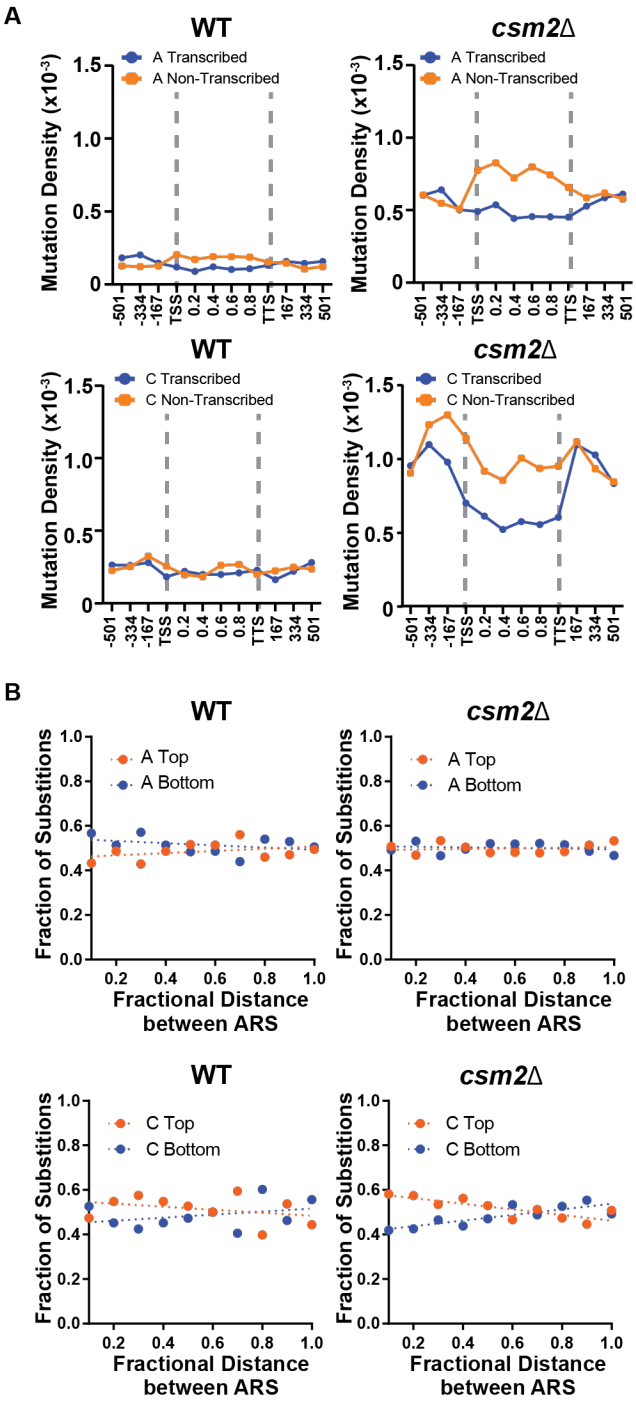

Figure 2. Transcriptional and Replicative Strand Biases of MMS-Induced Substitutions

(A) The density of A mutations (i.e. the fraction of A bases mutated) or C mutations on the transcribed (blue) and non-transcribed (orange) strand across yeast transcripts in WT and *csm2*Δ cells. Transcript regions were broken into fractional bins of 0.2 of the transcript length and the density of A or C mutations determined per bin. 3 additional bins of 500 bp each where also included upstream of the transcription start site (TSS) and downstream of the transcription termination site (TTS).

(B) The fraction of A and C mutations occurring on the top (orange) and bottom (blue) strands across replication units in the genomes of WT and *csm2*Δ cells. Replication units were broken into 0.1 fractional bins between neighboring origins of replication and the fraction of A mutations or C mutations associated with each strand were calculated per bin. The fraction of mutations for each strand across the replication unit was fitted with linear regression lines (dashed lines).

ALKBH2 expression rescues the MMS-induced phenotypes of Shu complex deficient cells

Based on the analysis of the mutation patterns, we hypothesized that the Shu complex promotes the error-free bypass of 3meC. 3meC can be repaired by the AlkB family of Fe(II)/α-Ketoglutarate-dependent dioxygenases (Fedeles, Singh et al., 2015). This family is conserved from bacteria to humans; however, no yeast homolog has been found. Therefore, as of yet it remains unknown how yeast tolerates and repairs the highly toxic 3meC. In humans, there are nine AlkB homologs with ALKBH2 and ALKBH3 are responsible for 3meC DNA repair (Fedeles et al., 2015, Yi & He, 2013). We, therefore, reasoned that ectopic expression of AlkB homologs would rescue the MMS-induced phenotypes observed in Shu complex deficient cells. To test this, we took advantage of the lack of an AlkB homolog in yeast by ectopically expressing human AlkB homologs, *ALKBH2*, or *ALKBH3*, in *csm2*Δ cells and analyzed their effect on MMS sensitivity. *ALKBH2* and *ALKBH3* were expressed under the constitutive GAP promoter using a low-copy CEN plasmid. We find that both *ALKBH2* and *ALKBH3* expression leads to a partial rescue of the growth defects observed in MMS-exposed *csm2Δ* cells, with *ALKBH2* showing a stronger rescue (**Figure 3A**). Therefore, we focused on *ALKBH2* for the remainder of the experiments. As expected, *ALKBH2* expression very mildly rescues the MMS sensitivity of WT cells (**Figure 3A**). The growth defect rescue observed in MMS-treated *csm2Δ* cells depends on ALKBH2's enzymatic activity since expression of an *ALKBH2* catalytic dead mutant (ALKBH2-V101R,F120E herein referred to as alkbh2-CD) (Monsen, Sundheim et al., 2010) does not rescue *csm2*Δ cell viability (**Figure 3B**). We confirmed that the inability of

alkbh2-CD to rescue *csm2*Δ cells was not due to lower protein expression (**Figure S2)**. These findings are not specific to *csm2*Δ as *ALKBH2* rescues the MMS sensitivity of the other Shu complex members to the same extent (**Figure 3C**). The effect of *ALKBH2* expression on *csm2*Δ cell viability is specific for MMS damage as *ALKBH2* expression does not rescue the known growth defect observed in UV-treated *csm2Δ rev3Δ* double mutant cells (Xu, Ball et al., 2013) (**Figure 3D**).

Next, we analyzed the effect of *ALKBH2* expression on *csm2Δ* cells acutely exposed to MMS. To do this, we treated *ALKBH2*-expressing WT or *csm2Δ* cultures with 0.1% MMS for 30 minutes. We then assessed cell survival by counting viable colonies after two days of growth. We observe that *ALKBH2* expression leads to a dose-dependent increase in the survival of *csm2Δ* cells, whereas in WT cells, survival is only mildly rescued (**Figure 3E**).

Since 3meC only occurs at ssDNA, which is a physiological intermediate of DNA replication, we reasoned that *ALKBH2* expression would preferentially rescue the survival of cells that are progressing through S-phase and therefore more vulnerable to 3meC-induced toxicity. To test this, we compared the survival of *ALKBH2*-expressing *csm2Δ* cells arrested in G1 in MMS containing media with *ALKBH2*-expressing *csm2Δ* cells progressing through S-phase. In agreement with our rationale, *ALKBH2* was found to rescue the survival phenotype only for cells progressing in the S phase of cell cycle (**Figure 3F**). This is consistent with previous data in human cells suggesting that *ALKBH2* functions preferentially in S-phase (Gilljam, Feyzi et al., 2009).

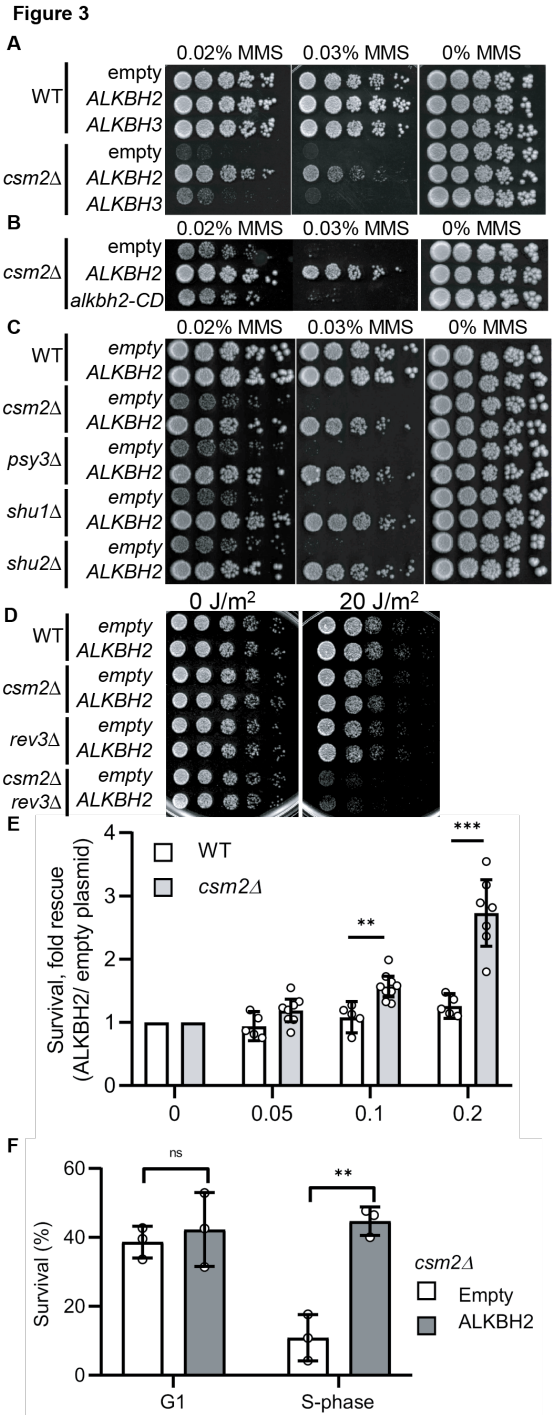

Figure 3. Expression of Human *ALKBH2* Rescues the MMS Sensitivity of *csm2Δ* Cells

(A) *csm2Δ* cells expressing *ALKBH2* exhibit decreased MMS sensitivity. Five-fold serial dilution of WT or *csm2*Δ cells transformed with an empty plasmid, a plasmid expressing *ALKBH2* or a plasmid expressing *ALKBH3* onto rich YPD medium or YPD medium containing the indicated MMS concentration were incubated for 2 days at 30 °C prior to being photographed.

(B) The enzymatic activity of ALKBH2 is required for the rescue of the MMS sensitivity of *csm2*Δ cells. *csm2*Δ cells transformed with an empty plasmid, a plasmid expressing *ALKBH2* or a plasmid expressing a

catalytic dead *ALKBH2* mutant were diluted and plated as described in (A) and incubated for three days at 30°C prior to being photographed.
(C) Expression of *ALKBH2* does not rescue the increased UV sensitivity observed in *csm2Δ rev3Δ* double mutants. Five-fold serial dilution of WT, *csm2Δ*, *rev3Δ*, or *rev3Δ csm2Δ* cells were transformed with an empty plasmid or a plasmid expressing *ALKBH2* and five-fold serially diluted onto rich YPD or rich YPD medium exposed to 20 J/m^2 ultra-violet (UV), and incubated for 2 days at 30 °C prior to being photographed. An untreated plate (0 J/m^2) serves as a loading control.
(D) *ALKBH2* expression rescues the MMS sensitivity of cells with deletions of the four Shu complex genes. WT, *csm2*Δ, *psy3*Δ, *shu1*Δ, or *shu2*Δ cells transformed with an empty plasmid, or a plasmid expressing *ALKBH2* were five-fold serially diluted, plated and analyzed as described in (B).
(E) *csm2Δ* cells expressing *ALKBH2* exhibit increased survival after acute MMS treatment. YPD liquid cultures of WT or *csm2*Δ cells transformed with an empty plasmid or a plasmid expressing *ALKBH2* were treated with the indicated concentration of MMS following plating onto rich YPD medium. Colony number was assessed after incubation for two days at 30°C. Fold rescue of cellular survival represents the ratio of the survival of cells expressing *ALKBH2* relative to the survival of cells expressing the empty plasmid. Survival represents the number of colonies as a percentage of the colonies obtained without MMS treatment. The individual and mean values from five to nine experiments were plotted. Error bars indicate 95% confidence intervals. The *p*-values between WT and *csm2*Δ cells treated with 0.1% MMS and 0.2% MMS were calculated using an unpaired two-tailed Student's t-test and were $p \leq 0.01$ and $p \leq 0.001$, respectively.
(F) S-phase *csm2*Δ cells expressing *ALKBH2* exhibit increased survival after acute MMS treatment. WT or *csm2*Δ cells were synchronized on G1 with alpha factor and either released from G1 arrest or maintained in G1 in the presence or absence of 0.1% MMS. Cells were plated after 30 minutes of treatment and the colony number was assessed after incubation for two days at 30°C. Survival is calculated as described in (E). The mean values from three experiments were plotted with standard deviations. The *p*-values between control (empty plasmid) and *ALKBH2* expressing cells were calculated using an unpaired two-tailed Student's t-test and were $p>0.05$ (n.s.) and $p \leq 0.001$ for the G1 and S-phase cells, respectively.

***ALKBH2* expression alleviates the MMS-induced mutations observed in Shu complex mutant, *csm2*Δ**

Since 3meC is a mutagenic lesion, we asked whether *ALKBH2* expression would alleviate the observed mutational load of MMS-exposed *csm2Δ* cells. To do this, we utilized the *CAN1* reporter assay. The *CAN1* gene encodes for an arginine permease, therefore when cells are exposed to the toxic arginine analog canavanine, only cells that acquire mutations in the *CAN1* gene grow. *ALKBH2* expression decreased the mutation rates in MMS-exposed *csm2Δ* cells (**Figure 4A**). This decreased mutation rate is specific for alkylation lesions as *ALKBH2* expression fails to rescue the increase in spontaneous mutations observed in a Shu complex

mutant, *csm2Δ* cells (**Figure 4A**). Furthermore, the rescue of *csm2*Δ mutation rate by *ALKBH2* depends on *ALKBH2* catalytic activity (**Figure S3**). These spontaneous mutations are likely due to the TLS-mediated bypass of AP sites (Ball et al., 2009, Godin et al., 2016c, Rosenbaum et al., 2019, Shor et al., 2005, Shrivastav et al., 2010). To determine whether the decrease in mutations in MMS-treated, *ALKBH2*-expressing *csm2Δ* cells corresponds to the repair of 3meC, we sequenced the *CAN1* gene of canavanine resistant clones. Can-R isolates from MMS-treated *csm2Δ* cells displayed frequent mutation of the *CAN1* gene with substitutions at A:T and C:G bases as well as single nucleotide deletions and complex events consisting of two mutations separated by less than 10 bp that are a signature of error-prone trans-lesion synthesis (Northam et al., 2010, Sakamoto et al., 2007). Accordingly, *ALKBH2* expression in *csm2Δ* cells decreased the frequency of deletions, complex mutations, and substitutions at C:G base pairs (**Figure 4B**). These findings support a model in which the Shu complex prevents the cytotoxicity and mutagenicity of 3meC and in its absence, yeast are reliant on TLS to bypass these lesions resulting an increase of C:G substitutions, small deletions, and complex mutations.

We previously demonstrated that the Shu complex preferentially binds to double-flap DNA substrates and has a two-fold higher affinity for double-flap DNA containing an AP site analog (Godin et al., 2016c, Rosenbaum et al., 2019). Therefore, we asked whether the DNA binding subunits of the Shu complex, Csm2-Psy3, would similarly have higher affinity for double-flap DNA containing 3MeC. To address this, we examined the affinity of recombinant Csm2-Psy3 to a FAM-labeled double-flap substrate in the presence or absence of 3meC by fluorescence anisotropy (**Figure 4C**). Indeed, Csm2-Psy3 has a two-fold improved affinity for a double-flap substrate containing a 3meC lesion on the ssDNA at the ssDNA/dsDNA junction relative to unmodified substrate [3meC, K_d= 5.1 ± 1.1; C, K_d= 11.1 ± 2.1; **Figure 4C**]. These

321 results suggest that the Shu complex increases error-free bypass of 3meC by preferentially

322 recognizing 3meC lesions on ssDNA in double-flap substrates.

Figure 4

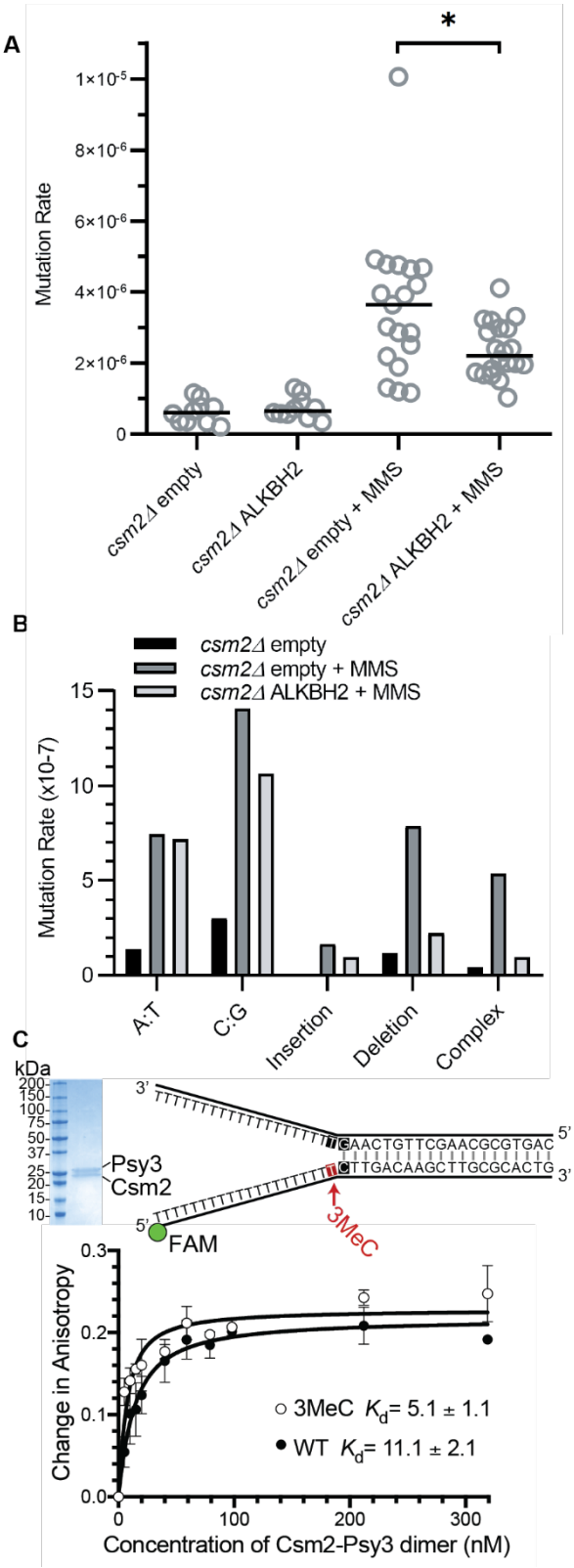

323

Figure 4. *ALKBH2* Expression Rescues the 3meC-Induced Mutagenesis Observed in MMS Exposed *csm2Δ* Cells

(A) *csm2Δ* cells expressing *ALKBH2* exhibit reduced MMS-induced mutation rate. Spontaneous and MMS-induced mutation rates at the *CAN1* locus were measured in *csm2*Δ cells transformed with an empty plasmid or a plasmid expressing *ALKBH2*. Each measurement (dots) and the median value of 10 to 20 experiments (horizontal bar) were plotted. The *p*-values between control (empty plasmid) and *ALKBH2* expressing cells were calculated using a Mann-Whitney Ranked sum test and were $p>0.05$ and $p < 0.03$ for the for the untreated and MMS treated samples respectively.

(B) Sequencing of the *CAN1* gene in canavanine resistant colonies was used to calculate the frequency of MMS-induced substitutions, insertions, deletions, and complex mutations in *csm2*Δ cells transformed with either an empty vector or *ALKBH2* expression vector. ALKBH2 expression significantly alters the MMS-induced mutation spectra ($p = 0.018$ by Chi-square analysis comparing the number of A:T substitutions, C:G substitutions, insertions, deletions, and complex mutations between MMS-treated *csm2*Δ cells containing an empty vector or *ALKBH2* expression vector). The spectrum contains a reduction in C:G substitutions, deletions, and complex mutations, while A:T substitutions and insertions are unchanged.

(C) The Csm2-Psy3 protein has high affinity for a double-flap DNA substrate containing a 3meC lesion. A Coomassie stained SDS-PAGE gel of recombinant Csm2-Psy3, which run at 27.7 kDa and 28 kDa, respectively. Equilibrium titrations were performed by titrating Csm2-Psy3 into the FAM-labeled double-flap substrate in the presence (4.53 nM 3meC) or absence (5.11 nM WT) of a 3meC at the indicated position and anisotropy was measured. Triplicate experiments were performed with standard deviations plotted. The data were fit to a quadratic equation (one-site binding model assumed) and dissociation constants (K_d) were calculated. Note the improved binding compared to previous studies (Rosenbaum et al., 2019) due to increased protein activity from improved constructs.

3meC repair in yeast is channeled through error-free post-replicative repair

The Shu complex directly functions with the canonical Rad51 paralogs, Rad55-Rad57, and Rad52 to promote HR through Rad51 filament formation (Gaines, Godin et al., 2015, Godin et al., 2013). In the context of error-free post-replicative repair, the Shu complex functions downstream of poly-ubiquitination of PCNA by Rad5-Ubc13-Mms2 (Xu et al., 2013). Therefore, we asked whether the rescue of the MMS-induced phenotypes by *ALKBH2* depends on Shu complex function as a Rad51 mediator. To address this question, we utilized a Csm2 mutant, *csm2-F46A*, that cannot stimulate Rad51 filament formation due to loss of its protein interaction with Rad55-Rad57 (Gaines et al., 2015, Godin et al., 2013). Suggesting that the Shu complex mediator function enables bypass of 3meC, we find that *ALKBH2* expression suppresses the MMS sensitivity of a *csm2-F46A* mutant to the same extent as a *csm2*Δ cell (**Figure 5A**). Next,

we asked whether the rescue of MMS sensitivity by *ALKBH2* would be observed in other HR mutants. To accomplish this, we ectopically expressed *ALKBH2* in cells with deletions of *CSM2, RAD51, RAD52, RAD55,* and *UBC13* and performed serial dilutions upon increasing-MMS dosage (**Figure 5B**). Surprisingly, *rad51*Δ*, rad52*Δ*,* and *rad55*Δ MMS sensitivity is not rescued by *ALKBH2* expression to the same extent as *csm2*Δ cells. In contrast, *ubc13*Δ MMS sensitivity is largely rescued by *ALKBH2* expression. This striking result suggests that the Shu complex functions primarily within Ubc13-initiated post-replicative repair pathway, while the canonical HR genes are also critical for the repair of DSBs induced by MMS through clustered lesions. Unlike Shu complex mutant cells, deletion of the canonical HR genes leaves cells vulnerable to toxic MMS-induced DSBs formed from lesions that are not subject to *ALKBH2* direct reversal.

To explore this idea further, we investigated the effect of *ALKBH2* in a *RAD55* phosphorylation mutant that is MMS sensitive while maintaining its DSB-repair proficiency (Herzberg, Bashkirov et al., 2006). In this *RAD55* mutant, three serine residues (2,8,14) are mutated to alanine residues (*rad55-S2,8,14A*). Since the *rad55-S2,8,14A* mutant cells largely phenocopy the defects observed in a Shu complex mutant (Herzberg et al., 2006), we asked whether Rad55 function in MMS-induced DNA damage may be uncoupled from its role in canonical DSB repair. Unlike *rad55*Δ cells, the *rad55-S2,8,14A* mutant MMS sensitivity is largely rescued by *ALKBH2* expression (**Figure 5C**). To further investigate the genetic relationship between the Shu complex and Rad55, we combined either *rad55*Δ or *rad55-S2,8,14A* with a *csm2*Δ mutant. As previously reported, *csm2*Δ *rad55*Δ double mutants exhibit the same MMS sensitivity as a *rad55*Δ mutant cell (Godin et al., 2013). In contrast, a *csm2*Δ *rad55-S2,8,14A* double mutant exhibits the same MMS sensitivity as a single *csm2*Δ cell (**Figure 5D**). This observation is surprising since the Shu complex is thought to function downstream of

Rad55. However, it is consistent with the specificity of the Shu complex in directly recognizing and enabling tolerance of MMS-induced DNA lesions (Rosenbaum et al., 2019).

Rad55 directly interacts with Csm2-Psy3 (Gaines et al., 2015, Godin et al., 2013). While Rad55-S2,8,14A mutant maintains its protein interactions with Rad57, Rad51, and Rad52, its interaction with the Shu complex has yet to be determined (Herzberg et al., 2006). Therefore, the Shu complex may help recruit Rad55 to specific MMS-induced DNA lesions through an interaction with phosphorylated Rad55 or at the interface where Rad55 is phosphorylated. To test this, we performed Y2H analysis of Rad55 or Rad55-S2,8,14S with Csm2 (**Figure 5E**). Interestingly, we observe a reduced interaction between Rad55-S2,8,14S with Csm2 (**Figure 5E**). These results suggest that Rad55 phosphorylation may stimulate its interaction with Csm2 or that Csm2 interacts with Rad55 in that region. In the context of MMS-induced DNA damage, our findings suggest that the Shu complex is likely contributing to the recognition of specific MMS-induced lesions and recruiting the HR machinery, such as Rad55-Rad57, to the lesion to facilitate their bypass and enable their repair following replication. Furthermore, other factors, such as a stalled replication fork, may also contribute to their recruitment.

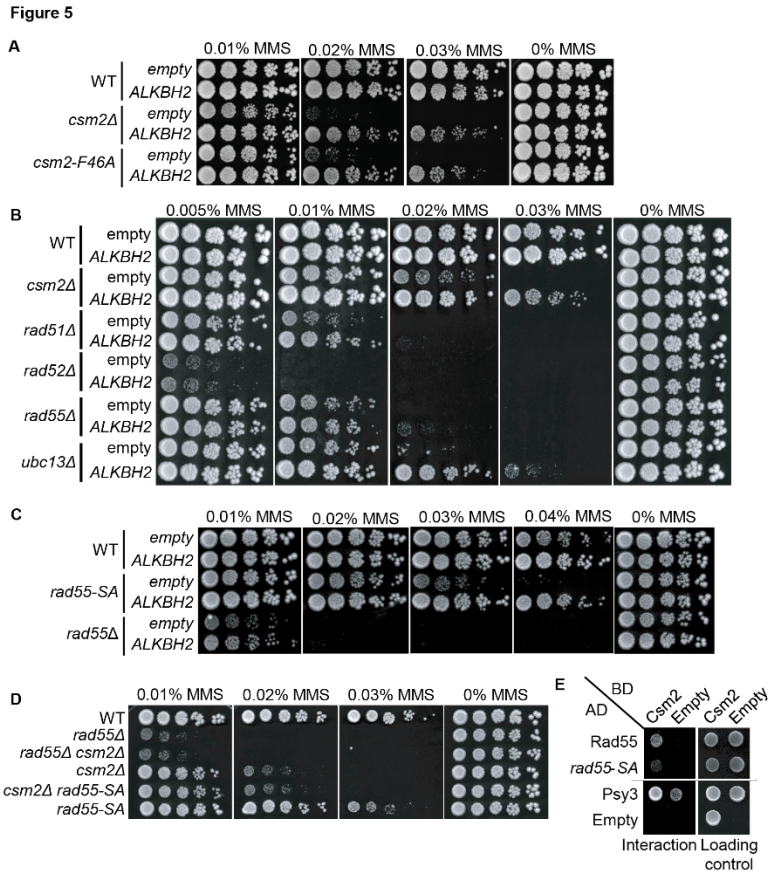

Figure 5. 3meC are Bypassed by the Error-Free Post Replicative Repair (PRR) Pathway

(A) *ALKBH2* rescues the MMS sensitivity of a *csm2-F46A* mutant, which is deficient for its Rad51 mediator activity. Five-fold serial dilution of WT, *csm2Δ*, or *csm2-F46A* cells were transformed with an empty plasmid or a plasmid expressing *ALKBH2* onto rich YPD medium or YPD medium containing the indicated MMS concentration and incubated for 3 days at 30°C prior to being photographed.

(B) Unlike PRR mutant *UBC13*, expression of *ALKBH2* mildly rescues the MMS sensitivity of HR factors, *RAD51, RAD52,* and *RAD55*. Five-fold serial dilution of WT, *csm2Δ*, *rad51Δ*, *rad52Δ*, *rad55Δ*, or *ubc13Δ* transformed with an empty plasmid or a plasmid expressing *ALKBH2* were five-fold serially diluted, plated, and analyzed as described in (A).

(C) *rad55-S2,8,14A* cells expressing *ALKBH2* exhibit decreased MMS sensitivity. WT, *rad55-S2,8,14A*, or *rad55Δ* cells transformed with an empty plasmid or a plasmid expressing *ALKBH2* were five-fold serially diluted, plated, and analyzed as described in (A).

(D) *csm2Δ* is epistatic to *rad55-S2,8,14A* for MMS damage. Cells with the indicated genotypes were five-fold serially diluted and plated as described in (A), and incubated for 2 days at 30°C prior to being photographed.

(E) rad55-S2,8,14A exhibit an impaired yeast-2-hybrid (Y2H) interaction with Csm2. Y2H analysis of pGAD-*RAD55*, *rad55-S2,8,14A*, *PSY3*, or pGAD-C1 (Empty) with pGBD-*RAD57*, *CSM2*, pGBD-C1 (Empty). A Y2H interaction is indicated by plating equal cell numbers on SC medium lacking histidine, tryptophan, and leucine. Equal cell loading is determined by plating on SC medium lacking tryptophan and leucine used to select for the pGAD (AD) and pGBD (BD) plasmids.

DISCUSSION

Among the many alkylation-induced DNA lesions, 3meC is well noted due to its cytotoxic and mutagenic impact during DNA replication (Nieminuszczy, Mielecki et al., 2009, Shrivastav et al., 2010, Sikora et al., 2010). In eukaryotes, the adduct is formed endogenously from S-adenosyl methionine (SAM) reactivity with DNA and from the enzymatic activity of DNA methyltransferases, and exogenously from alkylating agents such as nitrosamines, which are present in the tobacco smoke, temozolomide, or MMS (Chatterjee & Walker, 2017, Dango, Mosammaparast et al., 2011, Pataillot-Meakin, Pillay et al., 2016, Rosic, Amouroux et al., 2018). 3meC occurs primarily in ssDNA and can stall the replicative polymerases. Unlike bacteria and higher eukaryotes, yeast does not encode for an enzyme capable of directly repairing 3meC from ssDNA (Admiraal, Eyler et al., 2019, Sedgwick et al., 2007). Therefore, yeast rely on bypass mechanisms to complete DNA replication. Here, we utilized the budding yeast model to demonstrate that the Shu complex facilitates an HR-mediated error-free bypass of alkylation damage, including 3meC and AP sites, to prevent mutagenesis and toxicity.

The Shu complex is primarily involved in tolerance of replicative base-template damage, being dispensable for DSB repair (Ball et al., 2009, Godin et al., 2016c). This makes the Shu complex ideal to dissect the role of HR during bypass of specific base lesions. The major phenotypes observed in MMS-exposed Shu complex disrupted cells are decreased cell survival and elevated mutation frequency (Ball et al., 2009, Godin et al., 2016b, Shor et al., 2005). We observe that *ALKBH2* expression specifically alleviates the MMS-induced phenotypes of Shu complex disrupted cells (**Figures 3 and 4**). This *ALKBH2* rescue is partial, which is consistent with the Shu complex role in tolerance of another MMS-induced lesion, an AP site (Godin, Lee et al., 2016a, Rosenbaum et al., 2019). Although it is not possible to specifically induce 3meC, it

is possible to regulate the occurrence of its template, by controlling the amount of ssDNA in MMS-exposed cells. It would be interesting to observe how the rescue by expression of *ALKBH2* correlates with the amount of ssDNA. Consistently, our results show that *ALKBH2* is only able to rescue the MMS sensitivity of Shu complex mutant cells that are progressing through S-phase and therefore exhibit ssDNA intermediates (**Figure 3E**). Furthermore, we find that Shu complex members, Csm2-Psy3, have a higher binding affinity for a double-flap substrate containing 3meC lesions on the ssDNA lagging strand (**Figure 4C**).

The error-free PRR pathway requires polyubiquination of PCNA by Mms2-Ubc13-Rad5 and the activity of the core HR machinery (Branzei & Szakal, 2017, Xu, Blackwell et al., 2015). Interestingly, the deletion of other HR factors, such as *RAD51*, are only partially rescued by *ALKBH2* expression (**Figure 5B**). This can be explained by their critical role in DSB repair, an activity for which the Shu complex is largely dispensable. Our results are consistent with 3meC being bypassed by the HR branch of the PRR pathway (**Figure 6**) and the notion that the Shu complex is an HR factor specialized for replication-damage.

Figure 6

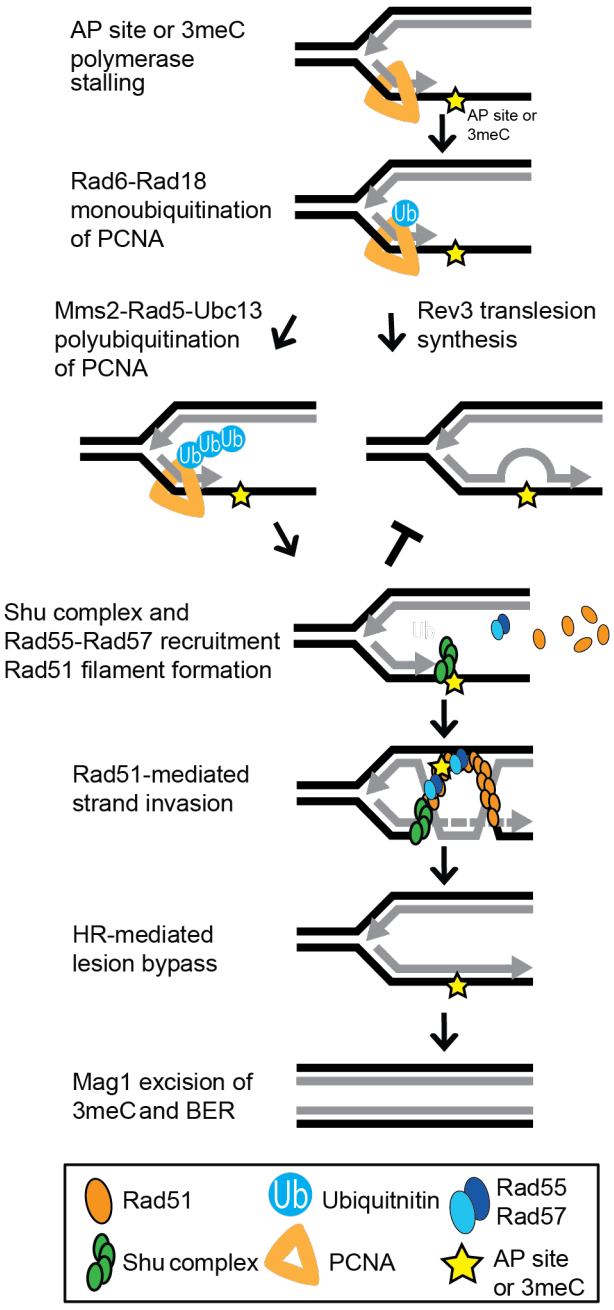

Figure 6. Model of Shu Complex-Mediated Error-Free Bypass of AP Sites and 3meC
MMS-induced AP sites and 3meC (yellow star) arising at DNA replication intermediates at ssDNA can stall the replicative polymerase. Replication fork stalling leads to PCNA (orange triangle) K63–linked polyubiquitination of lysine 164 (K164) by the sequential activities of the Rad6-Rad18 and Mms2-Rad5-Ubc18 complexes. The Shu complex (green ovals) through its DNA-binding components, Csm2-Psy3, binds to 3meC at a double-flap DNA junction to promote Rad55-Rad57 (blue ovals) recruitment and Rad51 filament formation (orange ovals). Thus, enabling Rad51-mediated HR with the newly synthesized sister chromatid. Importantly, the Shu complex activity prevents mutagenesis from TLS-mediated error-

prone bypass of 3meC. After DNA synthesis using the undamaged sister chromatid as template, the HR intermediates are resolved. The error-free bypass of 3meC enables S-phase completion in a timely manner. Finally, after replication is completed, 3meC are likely recognized and excised by the Mag1 glycosylase, which initiates the BER-mediated repair.

It is important to note that TLS can bypass 3meA directly and can also contribute to the mutation pattern observed for both WT and *csm2*Δ cells. Direct TLS bypass of 3meA leads to a mutation pattern of elevated A->T substitutions (Shrivastav et al., 2010). Therefore, we cannot rule out the contribution of direct TLS bypass of 3meA to the mutation pattern observed in our sequence analysis. However, previous work from our group has provided genetic, *in vivo*, and *in vitro* evidence of the Shu complex role in the error-free bypass of AP sites specifically (Godin 2016, Rosenbaum 2019).

AlkB proteins are also able to repair 1meA, which primarily occurs at ssDNA (Fedeles et al., 2015). Like 3meC, 1meA is a toxic and mutagenic adduct (Shrivastav et al., 2010). It possible that this lesion is also bypassed by the Shu complex and the error-free PRR pathway. Hence, we cannot rule out that ALKBH2 repair of 1meA may also contributes to the rescue of MMS-induced phenotypes that we observe. However, it is evident from our sequence analysis that the Shu complex contributes to the bypass of lesions occurring at G:C base pairs, which excludes 1meA. Moreover, 3meC is likely the main lesion contributing to mutagenesis from MMS at ssDNA (Saini et al., 2020, Yang et al., 2010).

A previous study claimed that yeast *TPA1* is an AlKB homolog (Shivange, Kodipelli et al., 2014). However, in our hands, and consistent with a recent report (Admiraal et al., 2019), *tpa1Δ* cells show no increased sensitivity to MMS. Furthermore, unlike other genes that are involved in repairing MMS-induced lesions, we find that *TPA1* does not exhibit a synthetic sick phenotype with Shu complex mutants upon MMS exposure (**Figure S4**). Recently, the Mag1 glycosylase was

491 shown to excise 3meC in dsDNA; therefore, initiating their repair through BER (Admiraal et al.,
492 2019). However, Mag1 cannot excise 3meCs from ssDNA (Admiraal et al., 2019). Whole genome
493 sequencing of MMS-treated *mag1*Δ yeast also contain primarily an elevation of substitutions at
494 A:T base pairs indicating that Mag1 activity in yeast contributes little to protecting against 3meC-
495 induced mutations. This is likely due to the restriction of these lesions to ssDNA and highlights
496 the need for a mechanism to bypass this lesion during DNA replication (**Figure 6**). Mag1 likely
497 plays a significant role in the removal of 3meC from dsDNA after its Shu complex-mediated
498 bypass allows replication to be completed (**Figure 6**).

499 Previous work from our group and others show that the Shu complex role is functionally
500 conserved in humans and mice (Abreu, Prakash et al., 2018, Martino & Bernstein, 2016,
501 Martino, Brunette et al., 2019). Additionally, human cells containing Shu complex deletions are
502 sensitive to MMS and DNA alkylating agents. Therefore, future studies will address whether the
503 human Shu complex functions as a back-up of the ALKBH enzymes in tolerating mutagenesis
504 and toxicity from 3meC. This is of particular importance since both *ALKBH2* and *ALKBH3* have
505 been proposed as tumor suppressors, being silenced in various tumors, including gastric and
506 breast cancer (Fedeles et al., 2015, Gao, Li et al., 2011, Knijnenburg, Wang et al., 2018,
507 Stefansson, Hermanowicz et al., 2017). On the other hand, *ALKBH3* is often overexpressed in
508 different cancers and inhibition of *ALKBH2* and *ALKBH3* can sensitize cancer cells to alkylating
509 chemotherapy (Choi, Jang et al., 2011, Koike, Ueda et al., 2012, Tasaki, Shimada et al., 2011,
510 Wang, Wu et al., 2015, Wu, Xu et al., 2011). Moreover, *ALKBH2* and *ALKBH3* upregulation
511 mediates resistance to chemotherapeutic agents such as temozolomide and *ALKBH3* loss leads to
512 endogenous 3meC accumulation in tumors cell lines (Cetica, Genitori et al., 2009, Dango et al.,
513 2011, Johannessen, Prestegarden et al., 2013). A connection between the human RAD51 paralog,

514 RAD51C, and ALKBH3 was recently described where RAD51C was important for recruitment
515 of ALKBH3 to DNA with 3meC. A role of the Shu complex promoting tolerance of 3meC could
516 provide a new avenue for therapeutic approaches to target these tumors.

517

518 **MATERIALS AND METHODS**

519 **Yeast strains, plasmids, and oligos**

520 The strains utilized are listed in **Supplemental Table 1** whereas all oligonucleotides used are
521 listed in **Supplemental Table 2**. The Y2H strains PJ69-4A and PJ69-4α were used as described
522 (Godin et al., 2013, James, Halladay et al., 1996). All strains are isogenic with W303 RAD5+
523 W1588-4C (Thomas & Rothstein, 1989) and W5059-1B (Zhao, Muller et al., 1998). KBY-1088-
524 3C (rad55-S2,8,14A) was generated by transformation of a cassette containing the 50 bp
525 homology upstream of the *RAD55* start codon and the rad55-S2,8,14A ORF fused to a kanMX6
526 resistance cassette and the 50 bp homology downstream of the *RAD55* stop codon. This fused
527 cassette was obtained using Gibson Assembly® Master Mix (NEB) following the manufacturer's
528 instructions and the primers used to generate the assembly fragments were designed using
529 NEBuilder Assembly Tool (https://nebuilder.neb.com). The rad55-S2,8,14A gene fragment was
530 commercially synthesized whereas the kanMX6 cassette was amplified from the pFA6a-kanMX6
531 plasmid (Longtine, McKenzie et al., 1998). Prior to transformation, the fused product was PCR
532 amplified using primers with 50nt of homology to the flanking regions of *RAD55* as described
533 (Longtine et al., 1998). All yeast transformations were performed as described (Sherman, Fink et
534 al., 1986). The integration of the rad55-S2,8,14A ORF was verified by PR amplification
535 followed by sequencing using the KanHisNat and Rad55.Check oligos as described in as

described (Longtine et al., 1998). pGAD-rad55-S2,8,14A was generated using Gibson Assembly® Master Mix (NEB) following the manufacturer's instructions and the primers used to generate the assembly fragments were designed using NEBuilder Assembly Tool (https://nebuilder.neb.com). ALKBH2 and ALKBH3 were cloned in the pAG416GPD-ccdB vector (Plasmid #14148 Addgene). pAG416GPD-ccdB-ALKBH2-CD was generated by site-directed mutagenesis of the pAG416GPD-ccdB-ALKBH2 plasmid as described (Zheng, Baumann et al., 2004) with minor adaptations according to the manufacturer's recommendations for PCR using Phusion High-Fidelity PCR Master Mix with HF Buffer (Thermo). All knock-outs were generated using the S1 and S2 primers and knock-out cassettes as described in (Longtine et al., 1998). All plasmids and strains were verified by DNA sequencing.

Chronic MMS Exposure and DNA Whole Genome Sequencing

Individual colonies of WT or *csm2Δ* cells were grown overnight at 30˚C. The cultures were then pinned onto YPD medium containing 0.008% MMS using a pinning robot from S&P Robotics. After a 2-day incubation at 30˚C the plates were replica-plated onto YPD plates containing 0.008% MMS using a robotic pinner, and then replated onto fresh YPD medium containing 0.008% MMS a total of 10 times. The MMS-exposed yeast were separated into single colonies (96 per strain). These colonies were inoculated in YPD cultures and grown overnight at 30˚C. Genomic DNA was extracted from each culture by resuspending the yeast pellets in lysis buffer (20 mM Tris-Cl, 200 mM LiAc, 1.5% SDS, pH7.4), incubating the yeast for 15 min at 70˚C, incubating on ice for 10 min, adding an equal volume of 4M NaCl, and centrifuging the samples at maximum speed for 30 minutes at 4˚C. The supernatant was then added to an equal volume of phenol:chloroform:isoamyl alcohol (PCI). An equal volume of isopropanol was added to the

559 aqueous phase of the PCI extraction. The DNA pellet was washed twice with 70% ethanol prior
560 to resuspending in 10 mM Tris 8 buffer. The DNA the subjected to Illumina whole genome
561 sequencing. 1 µg of genomic DNA per sample was sheared and used to generate libraries for
562 sequencing with a KAPA DNA HyperPrep kit. Multiplexed libraries were sequenced with 96
563 samples on a single lane of an Illumina Hiseq4000. Illumina reads were aligned to the Saccer3
564 S288C reference genome with CLC Genomics Workbench version 7.5. CLC Genomics
565 Workbench was also used to identify mutations from these alignments using methods similar to
566 those previously described (Sakofsky, Roberts et al., 2014). Briefly, mutations were identified as
567 differences from the reference genome that were greater than 9 reads covering the site, and for
568 which between 45-55% of the reads supported the mutation. Additionally, any mutations
569 occurring in multiple samples were removed from analyses as likely polymorphisms or
570 alignment artifacts. The complete list of mutations is provided in **Supplemental Table 3**. Raw
571 sequencing reads in fastq format have been submitted to the NCBI short read archive under
572 BioProject accession number PRJNA694993.

573

574 **Growth Assays**

575 Individual colonies of the indicated strains were transformed with an empty plasmid or a plasmid
576 expressing ALKBH2 as indicated. The cultures were grown in 3ml YPD or SC-URA medium
577 overnight at 30˚C. Five-fold serial dilutions were performed (Godin et al., 2016c) except that 5
578 µL of culture at 0.2 OD_{600} were 5-fold serially diluted onto YPD medium or YPD medium
579 containing the indicated MMS concentration. UV treatment was performed using Stratagene
580 Stratalinker 2400 UV Crosslinker. The plates were imaged after 48 h or 72 h of incubation at
581 30˚C and the brightness and contrast was globally adjusted using Photoshop (Adobe Systems

582 Incorporated).

583

584 **Protein Blotting**

585 Parental and *csm2*Δ cells were transformed with an empty plasmid or plasmid expressing either
586 ALKBH2 or ALKBH2-CD. The cultures were grown in SC-URA medium overnight at 30˚C.
587 Subsequently, equal cell numbers (1 ml 0.75 OD_{600}) from each culture were pelleted, supernatant
588 was removed, and washed once with ddH_2O and pelleted again. Protein was extracted from
589 whole cell lysates by TCA preparation as described in 51 µl of loading buffer (Knop et al. 1999).
590 The 13 µl of protein was run on a 10% SDS-PAGE gel and transferred to a PDVF membrane by
591 semidry transfer (Bio-Rad) at 13V for 90 min. ALKBH2 or Kar2 was Western blotted using
592 αALKBH2 antibody [AbCam (ab154859); 1:1000 with secondary antibody anti-rabbit (Jackson
593 ImmunoResearch Laboratories 1:10,000] or αKar2 antibody [Santa Cruz (sc-33630); 1:5000 with
594 secondary antibody anti-rabbit (Jackson ImmunoResearch Laboratories 1:10,000] as a loading
595 control.

596

597 **Survival Assays**

598 Individual colonies of WT or *csm2Δ* cells were transformed with an empty plasmid or a plasmid
599 expressing *ALKBH2* and grown in 3ml SC-URA medium at 30˚C overnight. The cultures were
600 diluted to 0.2 OD_{600} in 50 ml SC-URA medium and grown for 3-4 h at 30˚C. The cultures were
601 all diluted to 0.2 OD_{600} in YPD or YPD containing 0.05%, 0.1% or 0.2% MMS and incubated for
602 30 minutes at 30˚C. After the treatment, the cultures were washed twice with YPD and
603 resuspended to 0.2 OD_{600} in YPD. The cultures were diluted 1/10000 (untreated and 0.05%

MMS) or 1/1000 (0.1% and 0.2% MMS) and 150 ul were plated in YPD medium plates in duplicate. The plates were incubated at 30˚C for 2 days before imaging. The colonies were counted using OpenCFU (Geissmann, 2013). Data from 5 to 9 colonies from at least 3 independent transformants was used.

Canavanine Mutagenesis Assay

Individual colonies of the indicated strains were transformed with an empty plasmid or a plasmid expressing *ALKBH2* and grown in 3ml SC-URA medium or SC-URA medium containing 0.00033% MMS for 20 h at 30˚C. The cultures were diluted to 3.0 OD_{600}. 150 ul were plated on SC-ARG+CAN (0.006% canavanine) medium in duplicate or 150 ul of a 1:10,000 dilution were plated on SC medium in duplicate. The plates were then incubated for 48 hours at 30˚C before imaging. The colonies were counted using OpenCFU (Geissmann, 2013) to measure total cell number (SC) or forward mutation rates (SC-ARG+CAN). The mutation frequency was obtained by dividing colony number in SC-ARG+CAN by the number obtained in the SC plates times the dilution factor. Mutation frequencies were converted to mutation rates using methods described (Drake, 1991). Data from 10 to 20 colonies from at least three independent transformants was used. Differences in mutation rates were evaluated using a Mann-Whitney rank sum test comparing the independent rate measurements between untreated *csm2*Δ yeast expressing either an empty vector control or *ALKBH2* and between MMS-treated *csm2*Δ yeast expressing either an empty vector control or *ALKBH2*. Mutations occurring within the *CAN1* gene were identified by selecting independent canavanine resistant colonies, isolating genomic DNA from these samples, and PCR amplifying the *CAN1* gene from each isolate with primers containing unique barcodes (**Supplemental Table 4**). These PCR products were pooled and sequenced on a PacBio Sequel

627 sequencer as in (Hoopes et al., 2017). PacBio reads were separated by barcodes and aligned to
628 the *CAN1* gene sequence using Geneious software. Geneious was also used to identify mutations
629 among these alignments as differences from the reference *CAN1* sequence that are supported by
630 two or more independent reads that occur in greater than 30% of all reads for each sample. 452
631 out of 458 mutations identified were supported by greater than 50% of the reads for the sample.
632 All mutations identified by PacBio sequencing are provided in **Supplemental Table 5**.
633

634 **Yeast-Two-Hybrid Assays**

635 The yeast-two-hybrid experiments using the indicated pGAD and pGBD plasmids were
636 performed (Godin et al., 2013) except that both pGAD and pGBD plasmids were transformed
637 into PJ69-4A (James et al., 1996). A yeast-two-hybrid interaction is indicated by growth on
638 synthetic complete (SC) medium lacking histidine, tryptophan, and leucine whereas equal cell
639 loading was observed by plating the cells on SC medium lacking tryptophan and leucine to select
640 for the pGAD (leucine) or pGBD (tryptophan) plasmids.
641

642 **Csm2-Psy3 Purification**

643 The Csm2-Psy3 heterodimer was cloned into the dual expression plasmid pRSFDuet (EMD
644 Millipore) which encode a Strep-tagged Csm2 and FLAG-tagged Psy3. All affinity tags were
645 fused to the N-terminus of the protein. This plasmid was transformed into *E.coli* (Rosetta
646 P.LysS) and grown at 37°C until 0.6 OD_{600} and recombinant protein expression was induced by
647 addition of 0.5 mM isopropyl beta thiogalactoside (IPTG) at 18°C overnight for 16–18 h. Cells
648 were harvested by centrifugation and pellets were frozen at -80°C. Approximately 38 g of cell
649 pellet was lysed in 80 mL of lysis buffer containing 25 mM Tris (pH 7.4), 300 mM KCl, 10%

glycerol, 5 mM β-mercaptoethanol supplemented with protease inhibitors (Roche), 1mM PMSF, 1 mM $ZnCl_2$ and 0.01% IGEPAL CA-630. Cells were lysed using an emulsiflex and centrifuged at 15,000 × *g* for 1 h at 4°C. Lysed supernatant was incubated with 5 mL of ANTI-FLAG M2 affinity resin (Sigma) overnight and then washed in a solution consisting of 25 mM Tris (pH 7.4), 150 mM KCl, 10% glycerol, and 0.01% IGEPAL CA-630. To elute bound Csm2-Psy3, the wash buffer was supplemented with 0.1mg/mL 3X-FLAG peptide (Sigma). Elutions were then loaded onto a HiTrap Heparin HP (GE Healthcare) affinity chromatography. The complex was loaded onto the column and washed for 200 mL with (25 mM Tris (pH 7.4), 150 mM KCl, 1 mM DTT, 10% glycerol, and 0.01% IGEPAL CA-630). The complex was eluted with a gradient elution from 0% to 100% (25 mM Tris (pH 7.4), 150 mM KCl, 1 mM DTT, 10% glycerol, and 0.01% IGEPAL CA-630) over 20 mL. The Csm2-Psy3 protein typically eluted around 400–600 mM NaCl. Then, Csm2-Psy3 Heparin elutions were subsequently purified by size exclusion chromatography using a Sephacryl S200 column (GE Healthcare) in buffer (25 mM Tris (pH 7.4), 150 mM KCl, 1 mM DTT, 10% glycerol, and 0.01% IGEPAL CA-630) eluting as a single peak and visualized as heterodimers by SDS-PAGE electrophoresis. Csm2-Psy3 protein concentration was determined by BCA Assay as previously described (Rosenbaum et al., 2019).

Substrates for Fluorescence Anisotropy

WT	5'-CAGTGCGCAAGCTTGTCAAGTTTTTTTTTTTTTTTTTTT-3'
WTT-5'FAM	5'/56-FAM/TTTTTTTTTTTTTTTTTTTCCTTGACAAGCTTGCGCACTG-3'
3meC-5'FAM	5'/56-FAM/TTTTTTTTTTTTTTTTTTT/i3Me-dC/CTTGACAAGCTTGCGCACTG-3'

Equilibrium Fluorescence Anisotropy Assays

Anisotropy experiments were performed using a FluoroMax-3 spectrofluorometer (HORIBA Scientific) on and a Cary Eclipse Spectrophotometer. All substrates used for anisotropy

contained a 5'-FAM moity incorporated at the end of the single-stranded end of the fork (**Figure 4C**). Substrates either contained a thymidine (T) or 3meC at the double-flap junction in the ssDNA. Anisotropy measurements were recorded in a 150 µL cuvette containing 20 mM Tris pH 8.0 and 5.11 or 4.53 nM of FAM-labeled double-flap substrate as a premixed sample of purified Csm2-Psy3 protein and substrate (5.11 nM WT + 1.6 µM Csm2-Psy3 dimer in 50 nM NaCl) was titrated into the cuvette. Fluorescence anisotropy measurements were recorded using the integrated polarizer and excitation and emission wavelengths of 495 and 520 nm, respectively, with slit widths of 10 nm. Titrations were carried out at 25°C and were carried out until anisotropy became unchanged. All experiments were performed in triplicate. Dissociation constants (K_d) were calculated by fitting our data to a quadratic equation [$Y = M^* ((x + D + K_d) - \text{sqrt}(((x + D + K_d)^2) - (4*D*x)))/(2*D)$] assuming a one site binding model. Data were fit with PRISM7 software. Unprocessed raw anisotropy values are in the source data file.

ACKNOWLEDGEMENTS

This study was supported by the National Institutes of Health grant (ES030335 to K.A.B.; CA218112 to S.A.R.) and the American Cancer Society (129182-RSG-16-043-01-DMC to K.A.B. and 133947-PF-19-132-01-DMC to S.R.H.).

REFERENCES

Abreu CM, Prakash R, Romanienko PJ, Roig I, Keeney S, Jasin M (2018) Shu complex SWS1-SWSAP1 promotes early steps in mouse meiotic recombination. *Nat Commun* 9: 3961

692 Admiraal SJ, Eyler DE, Baldwin MR, Brines EM, Lohans CT, Schofield CJ, O'Brien PJ (2019) Expansion of
693 base excision repair compensates for a lack of DNA repair by oxidative dealkylation in budding yeast. *J*
694 *Biol Chem* 294: 13629-13637
695
696 Arbel M, Liefshitz B, Kupiec M (2020) DNA damage bypass pathways and their effect on mutagenesis in
697 yeast. *FEMS Microbiol Rev*
698
699 Ball LG, Zhang K, Cobb JA, Boone C, Xiao W (2009) The yeast Shu complex couples error-free post-
700 replication repair to homologous recombination. *Mol Microbiol* 73: 89-102
701
702 Beranek DT (1990) Distribution of methyl and ethyl adducts following alkylation with monofunctional
703 alkylating agents. *Mutat Res* 231: 11-30
704
705 Bjoras M, Klungland A, Johansen RF, Seeberg E (1995) Purification and properties of the alkylation repair
706 DNA glycosylase encoded the *MAG* gene from *Saccharomyces cerevisiae*. *Biochemistry* 34: 4577-4582
707
708 Boiteux S, Jinks-Robertson S (2013) DNA repair mechanisms and the bypass of DNA damage in
709 *Saccharomyces cerevisiae*. *Genetics* 193: 1025-1064
710
711 Branzei D, Szakal B (2017) Building up and breaking down: mechanisms controlling recombination during
712 replication. *Crit Rev Biochem Mol Biol* 52: 381-394
713
714 Broomfield S, Chow BL, Xiao W (1998) MMS2, encoding a ubiquitin-conjugating-enzyme-like protein, is a
715 member of the yeast error-free postreplication repair pathway. *Proc Natl Acad Sci U S A* 95: 5678-83
716
717 Cetica V, Genitori L, Giunti L, Sanzo M, Bernini G, Massimino M, Sardi I (2009) Pediatric brain tumors:
718 mutations of two dioxygenases (hABH2 and hABH3) that directly repair alkylation damage. *J Neurooncol*
719 94: 195-201
720
721 Chan K, Resnick MA, Gordenin DA (2013) The choice of nucleotide inserted opposite abasic sites formed
722 within chromosomal DNA reveals the polymerase activities participating in translesion DNA synthesis.
723 *DNA Repair (Amst)* 12: 878-89
724
725 Chatterjee N, Walker GC (2017) Mechanisms of DNA damage, repair, and mutagenesis. *Environ Mol*
726 *Mutagen* 58: 235-263
727
728 Choi SY, Jang JH, Kim KR (2011) Analysis of differentially expressed genes in human rectal carcinoma
729 using suppression subtractive hybridization. *Clin Exp Med* 11: 219-26
730
731 Dango S, Mosammaparast N, Sowa ME, Xiong LJ, Wu F, Park K, Rubin M, Gygi S, Harper JW, Shi Y (2011)
732 DNA unwinding by ASCC3 helicase is coupled to ALKBH3-dependent DNA alkylation repair and cancer
733 cell proliferation. *Mol Cell* 44: 373-84
734
735 Drake JW (1991) A constant rate of spontaneous mutation in DNA-based microbes. *Proc Natl Acad Sci U*
736 *S A* 88: 7160-4
737

738 Fedeles BI, Singh V, Delaney JC, Li D, Essigmann JM (2015) The AlkB Family of Fe(II)/alpha-Ketoglutarate-
739 dependent Dioxygenases: Repairing Nucleic Acid Alkylation Damage and Beyond. *J Biol Chem* 290:
740 20734-42
741
742 Fu D, Calvo JA, Samson LD (2012) Balancing repair and tolerance of DNA damage caused by alkylating
743 agents. *Nat Rev Cancer* 12: 104-120
744
745 Gaines WA, Godin SK, Kabbinavar FF, Rao T, VanDemark AP, Sung P, Bernstein KA (2015) Promotion of
746 presynaptic filament assembly by the ensemble of *S. cerevisiae* Rad51 paralogues with Rad52. *Nat*
747 *Commun* 6: 7834
748
749 Gao W, Li L, Xu P, Fang J, Xiao S, Chen S (2011) Frequent down-regulation of hABH2 in gastric cancer and
750 its involvement in growth of cancer cells. *J Gastroenterol Hepatol* 26: 577-84
751
752 Geissmann Q (2013) OpenCFU, a new free and open-source software to count cell colonies and other
753 circular objects. *PLoS ONE* 8: e54072
754
755 Gilljam KM, Feyzi E, Aas PA, Sousa MM, Muller R, Vagbo CB, Catterall TC, Liabakk NB, Slupphaug G,
756 Drablos F, Krokan HE, Otterlei M (2009) Identification of a novel, widespread, and functionally important
757 PCNA-binding motif. *J Cell Biol* 186: 645-54
758
759 Godin S, Wier A, Kabbinavar F, Bratton-Palmer DS, Ghodke H, Van Houten B, VanDemark AP, Bernstein
760 KA (2013) The Shu complex interacts with Rad51 through the Rad51 paralogues Rad55-Rad57 to
761 mediate error-free recombination. *Nucleic Acids Res* 41: 4525-4534
762
763 Godin SK, Lee AG, Baird JM, Herken BW, Bernstein KA (2016a) Tryptophan biosynthesis is important for
764 resistance to replicative stress in *Saccharomyces cerevisiae*. *Yeast* 33: 183-9
765
766 Godin SK, Meslin C, Kabbinavar F, Bratton-Palmer DS, Hornack C, Mihalevic MJ, Yoshida K, Sullivan M,
767 Clark NL, Bernstein KA (2015) Evolutionary and Functional Analysis of the Invariant SWIM Domain in the
768 Conserved Shu2/SWS1 Protein Family from *Saccharomyces cerevisiae* to *Homo sapiens*. *Genetics* 199:
769 1023-33
770
771 Godin SK, Sullivan MR, Bernstein KA (2016b) Novel insights into RAD51 activity and regulation during
772 homologous recombination and DNA replication. *Biochem Cell Biol* 94: 407-418
773
774 Godin SK, Zhang Z, Westmoreland JW, Lee AG, Mihalevic MJ, Yu Z, Sobol RW, Resnick MA, Bernstein KA
775 (2016c) The Shu complex promotes error-free tolerance of alkylation-induced base-excision repair
776 products. *Nucleic Acids Res* 30: 8199-8215
777
778 Haracska L, Unk I, Johnson RE, Johansson E, Burgers PM, Prakash S, Prakash L (2001) Roles of yeast DNA
779 polymerases delta and zeta and of Rev1 in the bypass of abasic sites. *Genes Dev* 15: 945-954
780
781 Herzberg K, Bashkirov VI, Rolfsmeier M, Haghnazari E, McDonald WH, Anderson S, Bashkirova EV, Yates
782 JR, 3rd, Heyer WD (2006) Phosphorylation of Rad55 on serines 2, 8, and 14 is required for efficient
783 homologous recombination in the recovery of stalled replication forks. *Mol Cell Biol* 26: 8396-8409
784

785 Hoopes JI, Hughes AL, Hobson LA, Cortez LM, Brown AJ, Roberts SA (2017) Avoidance of APOBEC3B-
786 induced mutation by error-free lesion bypass. *Nucleic Acids Res* 45: 5243-5254
787
788 Huang ME, Rio AG, Nicolas A, Kolodner RD (2003) A genomewide screen in *Saccharomyces cerevisiae* for
789 genes that suppress the accumulation of mutations. *Proc Natl Acad Sci U S A* 100: 11529-34
790
791 James P, Halladay J, Craig EA (1996) Genomic libraries and a host strain designed for highly efficient two-
792 hybrid selection in yeast. *Genetics* 144: 1425-36
793
794 Johannessen TC, Prestegarden L, Grudic A, Hegi ME, Tysnes BB, Bjerkvig R (2013) The DNA repair protein
795 ALKBH2 mediates temozolomide resistance in human glioblastoma cells. *Neuro Oncol* 15: 269-78
796
797 Knijnenburg TA, Wang L, Zimmermann MT, Chambwe N, Gao GF, Cherniack AD, Fan H, Shen H, Way GP,
798 Greene CS, Liu Y, Akbani R, Feng B, Donehower LA, Miller C, Shen Y, Karimi M, Chen H, Kim P, Jia P et al.
799 (2018) Genomic and Molecular Landscape of DNA Damage Repair Deficiency across The Cancer Genome
800 Atlas. *Cell Rep* 23: 239-254 e6
801
802 Knop M, Siegers K, Pereira G, Zachariae W, Winsor K, Schiebel E (1999) Epitope tagging of yeast genes
803 using a PCR-based strategy: more tages and improved practical routines. *Yeast* 15(10B):963-72
804
805 Koike K, Ueda Y, Hase H, Kitae K, Fusamae Y, Masai S, Inagaki T, Saigo Y, Hirasawa S, Nakajima K, Ohshio
806 I, Makino Y, Konishi N, Yamamoto H, Tsujikawa K (2012) Anti-tumor effect of AlkB homolog 3 knockdown
807 in hormone- independent prostate cancer cells. *Curr Cancer Drug Targets* 12: 847-56
808
809 Longtine MS, McKenzie A, 3rd, Demarini DJ, Shah NG, Wach A, Brachat A, Philippsen P, Pringle JR (1998)
810 Additional modules for versatile and economical PCR-based gene deletion and modification in
811 *Saccharomyces cerevisiae*. *Yeast* 14: 953-61
812
813 Mao P, Brown AJ, Malc EP, Mieczkowski PA, Smerdon MJ, Roberts SA, Wyrick JJ (2017) Genome-wide
814 maps of alkylation damage, repair, and mutagenesis in yeast reveal mechanisms of mutational
815 heterogeneity. *Genome Res* 27: 1674-1684
816
817 Martino J, Bernstein KA (2016) The Shu complex is a conserved regulator of homologous recombination.
818 *FEMS Yeast Res* 16
819
820 Martino J, Brunette GJ, Barroso-Gonzalez J, Moiseeva TN, Smith CM, Bakkenist CJ, O'Sullivan RJ,
821 Bernstein KA (2019) The human Shu complex functions with PDS5B and SPIDR to promote homologous
822 recombination. *Nucleic Acids Res* 47: 10151-10165
823
824 Monsen VT, Sundheim O, Aas PA, Westbye MP, Sousa MM, Slupphaug G, Krokan HE (2010) Divergent ss-
825 hairpins determine double-strand versus single-strand substrate recognition of human AlkB-homologues
826 2 and 3. *Nucleic Acids Res* 38: 6447-55
827
828 Nieminuszczy J, Mielecki D, Sikora A, Wrzesinski M, Chojnacka A, Krwawicz J, Janion C, Grzesiuk E (2009)
829 Mutagenic potency of MMS-induced 1meA/3meC lesions in E. coli. *Environ Mol Mutagen* 50: 791-9
830
831 Northam MR, Robinson HA, Kochenova OV, Shcherbakova PV (2010) Participation of DNA polymerase ζ
832 in replication of undamaged DNA in *Saccharomyces cerevisiae*. *Genetics* 184: 27-42

Pataillot-Meakin T, Pillay N, Beck S (2016) 3-methylcytosine in cancer: an underappreciated methyl lesion? *Epigenomics* 8: 451-4

Roberts SA, Sterling J, Thompson C, Harris S, Mav D, Shah R, Klimczak LJ, Kryukov GV, Malc E, Mieczkowski PA, Resnick MA, Gordenin DA (2012) Clustered mutations in yeast and in human cancers can arise from damaged long single-strand DNA regions. *Mol Cell* 46: 424-35

Rosenbaum JC, Bonilla B, Hengel SR, Mertz TM, Herken BW, Kazemier HG, Pressimone CA, Ratterman TC, MacNary E, De Magis A, Kwon Y, Godin SK, Van Houten B, Normolle DP, Sung P, Das SR, Paeschke K, Roberts SA, VanDemark AP, Bernstein KA (2019) The Rad51 paralogs facilitate a novel DNA strand specific damage tolerance pathway. *Nat Commun* 10: 3515

Rosic S, Amouroux R, Requena CE, Gomes A, Emperle M, Beltran T, Rane JK, Linnett S, Selkirk ME, Schiffer PH, Bancroft AJ, Grencis RK, Jeltsch A, Hajkova P, Sarkies P (2018) Evolutionary analysis indicates that DNA alkylation damage is a byproduct of cytosine DNA methyltransferase activity. *Nat Genet* 50: 452-459

Saini N, Gordenin DA (2020) Hypermutation in single-stranded DNA. *DNA Repair (Amst)* 91-92: 102868
Saini N, Sterling JF, Sakofsky CJ, Giacobone CK, Klimczak LJ, Burkholder AB, Malc EP, Mieczkowski PA, Gordenin DA (2020) Mutation signatures specific to DNA alkylating agents in yeast and cancers. *Nucleic Acids Res* 48: 3692-3707

Sakamoto AN, Stone JE, Kissling GE, McCulloch SD, Pavlov YI, Kunkel TA (2007) Mutator alleles of yeast DNA polymerase ζ. *DNA Repair* 6: 1829-38.

Sakofsky CJ, Roberts SA, Malc E, Mieczkowski PA, Resnick MA, Gordenin DA, Malkova A (2014) Break-induced replication is a source of mutation clusters underlying kataegis. *Cell Rep* 7: 1640-1648
Sedgwick B, Bates PA, Paik J, Jacobs SC, Lindahl T (2007) Repair of alkylated DNA: recent advances. *DNA Repair (Amst)* 6: 429-42

Sherman F, Fink GR, Hicks JB (1986) *Methods in Yeast Genetics*. Cold Spring Harbor Laboratory Press, Cold Spring Harbor, NY

Shivange G, Kodipelli N, Monisha M, Anindya R (2014) A role for Saccharomyces cerevisiae Tpa1 protein in direct alkylation repair. *J Biol Chem* 289: 35939-52

Shor E, Weinstein J, Rothstein R (2005) A genetic screen for top3 suppressors in *Saccharomyces cerevisiae* identifies *SHU1, SHU2, PSY3* and *CSM2*: four genes involved in error-free DNA repair. *Genetics* 169: 1275-89

Shrivastav N, Li D, Essigmann JM (2010) Chemical biology of mutagenesis and DNA repair: cellular responses to DNA alkylation. *Carcinogenesis* 31: 59-70

Sikora A, Mielecki D, Chojnacka A, Nieminuszczy J, Wrzesinski M, Grzesiuk E (2010) Lethal and mutagenic properties of MMS-generated DNA lesions in Escherichia coli cells deficient in BER and AlkB-directed DNA repair. *Mutagenesis* 25: 139-47

Sobol RW, Kartalou M, Almeida KH, Joyce DF, Engelward BP, Horton JK, Prasad R, Samson LD, Wilson SH (2003) Base excision repair intermediates induce p53-independent cytotoxic and genotoxic responses. *J Biol Chem* 278: 39951-39959

Stefansson OA, Hermanowicz S, van der Horst J, Hilmarsdottir H, Staszczak Z, Jonasson JG, Tryggvadottir L, Gudjonsson T, Sigurdsson S (2017) CpG promoter methylation of the ALKBH3 alkylation repair gene in breast cancer. *BMC Cancer* 17: 469

Swanson RL, Morey NJ, Doetsch PW, Jinks-Robertson S (1999) Overlapping specificities of base excision repair, nucleotide excision repair, recombination, and translesion synthesis pathways for DNA base damage in Saccharomyces cerevisiae. *Mol Cell Biol* 19: 2929-2935

Tasaki M, Shimada K, Kimura H, Tsujikawa K, Konishi N (2011) ALKBH3, a human AlkB homologue, contributes to cell survival in human non-small-cell lung cancer. *Br J Cancer* 104: 700-6

Thomas BJ, Rothstein R (1989) Elevated recombination rates in transcriptionally active DNA. *Cell* 56: 619-30

Ulrich HD (2007) Conservation of DNA damage tolerance pathways from yeast to humans. *Biochem Soc Trans* 35: 1334-7

Wang P, Wu J, Ma S, Zhang L, Yao J, Hoadley KA, Wilkerson MD, Perou CM, Guan KL, Ye D, Xiong Y (2015) Oncometabolite D-2-Hydroxyglutarate Inhibits ALKBH DNA Repair Enzymes and Sensitizes IDH Mutant Cells to Alkylating Agents. *Cell Rep* 13: 2353-2361

Wu SS, Xu W, Liu S, Chen B, Wang XL, Wang Y, Liu SF, Wu JQ (2011) Down-regulation of ALKBH2 increases cisplatin sensitivity in H1299 lung cancer cells. *Acta Pharmacol Sin* 32: 393-8

Wyatt MD, Allan JM, Lau AY, Ellenberger TE, Samson LD (1999) 3-methyladenine DNA glycosylases: structure, function, and biological importance. *Bioessays* 21: 668-76

Wyatt MD, Pittman DL (2006) Methylating agents and DNA repair responses: Methylated bases and sources of strand breaks. *Chem Res Toxicol* 19: 1580-94

Xu X, Ball L, Chen W, Tian X, Lambrecht A, Hanna M, Xiao W (2013) The yeast Shu complex utilizes homologous recombination machinery for error-free lesion bypass via physical interaction with a Rad51 paralogue. *PLoS ONE* 8: e81371

Xu X, Blackwell S, Lin A, Li F, Qin Z, Xiao W (2015) Error-free DNA-damage tolerance in Saccharomyces cerevisiae. *Mutat Res Rev Mutat Res* 764: 43-50

Yang Y, Gordenin DA, Resnick MA (2010) A single-strand specific lesion drives MMS-induced hyper-mutability at a double-strand break in yeast. *DNA Repair (Amst)* 9: 914-21

Yi C, He C (2013) DNA repair by reversal of DNA damage. *Cold Spring Harb Perspect Biol* 5: a012575

Zhao X, Muller EG, Rothstein R (1998) A suppressor of two essential checkpoint genes identifies a novel protein that negatively affects dNTP pools. *Mol Cell* 2: 329-40

928 Zheng L, Baumann U, Reymond JL (2004) An efficient one-step site-directed and site-saturation
929 mutagenesis protocol. *Nucleic Acids Res* 32: e115

930

931 # SUPPLEMENTAL FIGURES

Figure S1

932 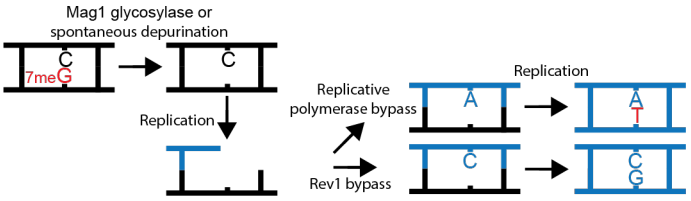

933 **Supplemental Figure 1. Schematic of How 7meG Derived AP Sites Lead to G to T as the Main**
934 **Substitution Pattern**
935 7meG can be converted to AP sites by spontaneous hydrolysis or the glycosylase activity of Mag1. AP
936 may be bypassed by the TLS activity of Rev1 which is this case is error-free. Alternatively, lesion bypass
937 by the replicative polymerase, which predominantly incorporates A across AP sites, would result in a G to
938 T mutation pattern.
939
940

941

942

943

944

945

946

947

948

949

Figure S2

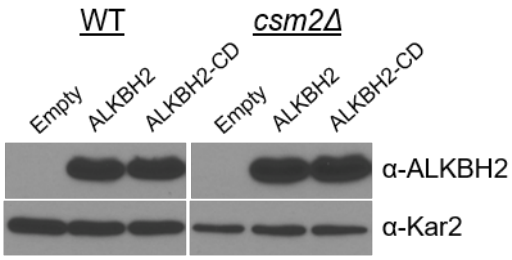

Supplemental Figure 2. Protein Blot Analysis of ALKBH2 and ALKBH2-CD Expression in WT and *csm2*Δ Cells.

WT and *csm2*Δ strains expressing an empty plasmid (pAG416GPD-ccdB) or a plasmid (pAG416GPD-ccdB) expressing either ALKBH2 or ALKBH2-CD were analyzed for ALKBH2 protein levels. Protein extracts from equal cell numbers were analyzed by western blot for ALKBH2 (α-ALKBH2) or Kar2 (α-Kar2) expression as a loading control.

Figure S3

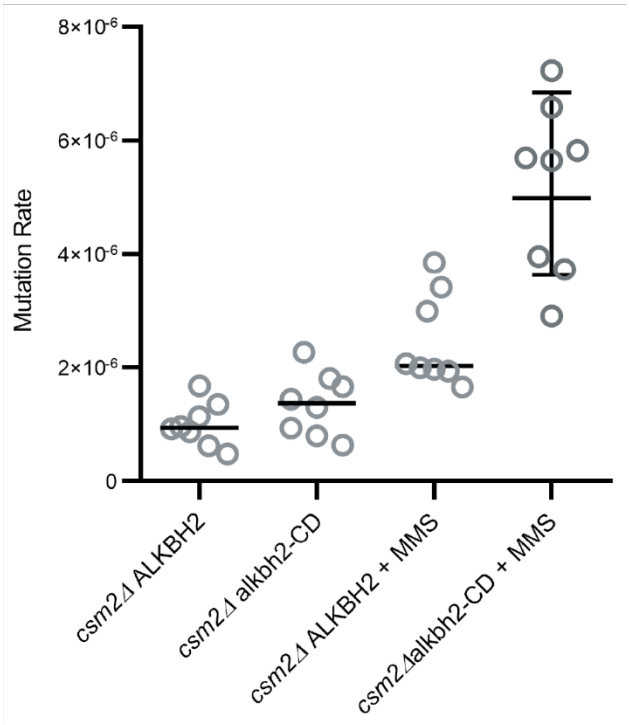

Supplemental Figure 3. Expression of a *ALKBH2* Catalytic Dead Mutant Does Not Rescue the Mutagenesis Observed in MMS Exposed *csm2Δ* Cells

csm2Δ cells expressing *ALKBH2-CD* exhibit an increased MMS-induced mutation rate. Spontaneous and MMS-induced mutation rates at the *CAN1* locus were measured in *csm2*Δ cells transformed with either a plasmid expressing *ALKBH2* or *ALKBH2-CD*. Each measurement (dots) and the median value of 8 experiments (horizontal bar) were plotted. The *p*-values between *ALKBH2* and *ALKBH2-CD* expressing cells were calculated using a Mann-Whitney Ranked sum test and were $p > 0.05$ and $p < 0.03$ for the for the untreated and MMS treated samples, respectively.

Figure S4

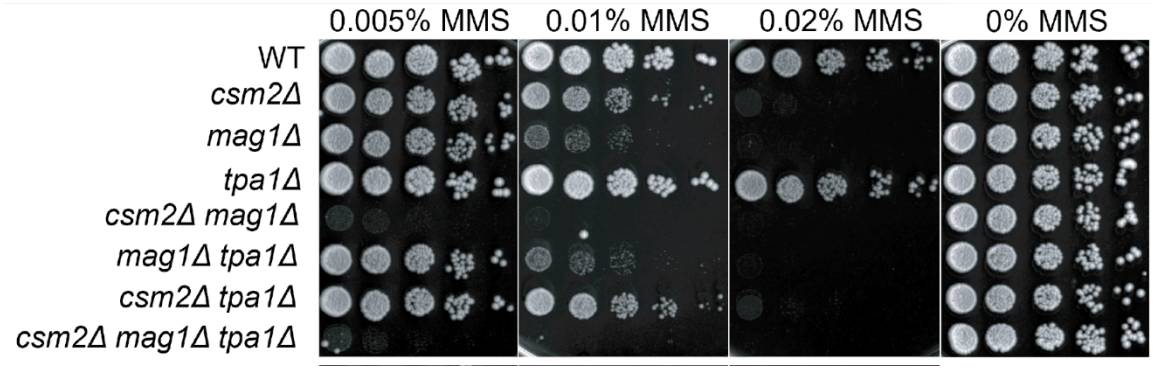

Supplemental Figure 4. *TPA1* Does Not Genetically Interact with *CSM2* or *MAG1* for MMS Damage

Five-fold serial dilution of cells with the indicated genotypes were transformed onto rich YPD medium or rich YPD medium containing the indicated MMS concentration were incubated for two days at 30°C prior to being photographed.